Microbioreactor arrays with integrated mixers and fluid injectors for high-throughput experimentation with pH and dissolved oxygen control†

Harry L. T. Lee,[a] Paolo Boccazzi,[b] Rajeev J. Ram*[a] and Anthony J. Sinskey*[b]

Received 6th June 2006, Accepted 3rd July 2006
First published as an Advance Article on the web 27th July 2006
DOI: 10.1039/b608014f

We have developed an integrated array of microbioreactors, with 100 μL working volume, comprising a peristaltic oxygenating mixer and microfluidic injectors. These integrated devices were fabricated in a single chip and can provide a high oxygen transfer rate ($k_La \approx 0.1\ s^{-1}$) without introducing bubbles, and closed loop control over dissolved oxygen and pH (±0.1). The system was capable of supporting eight simultaneous *Escherichia coli* fermentations to cell densities greater than 13 g-dcw L^{-1} (1 cm $OD_{650nm} > 40$). This cell density was comparable to that achieved in a 4 litre reference fermentation, conducted with the same strain, in a bench scale stirred tank bioreactor and is more than four times higher than cell densities previously achieved in microbioreactors. Bubble free oxygenation permitted near real time optical density measurements which could be used to observe subtle changes in the growth rate and infer changes in the state of microbial genetic networks. Our system provides a platform for the study of the interaction of microbial populations with different environmental conditions, which has applications in basic science and industrial bioprocess development. We leverage the advantages of microfluidic integration to deliver a disposable, parallel bioreactor in a single chip, rather than robotically multiplexing independent bioreactors, which opens a new avenue for scaling small scale bioreactor arrays with the capabilities of bench scale stirred tank reactors.

Introduction

Commonly used microbial cell culture tools have remained largely unchanged for the past few decades. Microbiologists have long had to compromise between the throughput and capabilities of the shaken microtiter plate, shake flasks, and stirred tank bioreactor. While conventional high throughput methods, such as shaken microtiter plates or flasks, offer the advantage of high parallelism, they suffer from a lack of control over pH and low oxygen transfer capacity. In contrast, bench scale stirred tank bioreactors offer full control over culture conditions and high oxygen transfer capacity; however these systems are labor intensive, complicated, and costly to operate in parallel. For applications such as industrial bioprocess development or scientific studies of microbial cells at high cell density, both high-throughput and the capacity for high cell density growth under controlled conditions are desirable.

In bioprocess development, a multitude of experiments are performed to screen for the best performing microbial strains and also to optimize growth conditions. High-throughput experiments using conventional technologies suffer from uncontrolled conditions and are not able to access the same physiological range encountered in production scale bioreactors. Therefore the best strains and nutrient combinations derived from these experiments require additional validation and optimization under controlled conditions in a series of time consuming and labor intensive bench scale stirred tank bioreactor experiments.[1]

For scientific study of microbial cells, especially in the area of understanding regulatory networks and the processing of environmental signals, growth under different environmental conditions is necessary to probe the response of the system and controlled conditions are essential for data interpretation. One example is quorum sensing where gene regulation depends on cell density dependent chemical signals.[2] In order to isolate cell density dependent effects, growth under controlled conditions is essential, as is ensuring that there are no hidden nutrient limitations in the medium.[3] Identifying potential nutrient limitations requires conducting multiple medium optimization experiments under high cell density conditions and looking for telltale changes in the growth rate. This is not possible with shake flask cultures and is quite difficult, even with stirred tanks due to the difficulty in measuring small changes in growth rate.

Recent efforts to address the need for a parallel bioreactor system with the capabilities of a stirred tank reactor have focused on improving the oxygen transfer rate of microtiter plates,[4] improving the control capabilities of shake flasks,[5] improving the parallelism of stirred tank bioreactors,[6–12] or developing microfabricated bioreactor systems,[13–19] as summarized in Table 1. Each of these approaches has addressed parallelism, oxygenation, control, automation, and scalability to various degrees. Of these approaches, the miniature arrays of stirred tanks with robotic fluid handling[10,11] have achieved

[a]*Research Laboratory of Electronics, Massachusetts Institute of Technology, 77 Massachusetts Ave, Cambridge, MA, 02139, USA. E-mail: rajeev@mit.edu*
[b]*Department of Biology and Health Sciences and Technology, 77 Massachusetts Ave, Cambridge, MA, 02139, USA. E-mail: asinskey@mit.edu*

† Electronic supplementary information (ESI) available: The measurement techniques, the oxygen transfer coefficient calculation, the fabrication process and a movie illustrating the mixing pattern. See DOI: 10.1039/b608014f

Table 1 Summary of miniature bioreactors for parallel operation. The first group are enhanced microtiter plates and flasks, the second group are miniature stirred tank systems, and the third group are microbioreactors

Type	Reference	Max cell density[15]/ g-dcw L^{-1}	k_La/s^{-1}	Working volume/mL	Parallelism	Controlled parameters	Comments
Oxygenated microplate	Duetz[4]	N.R.	0.05	0.20	96	*T*	Manual sampling for OD
pH controlled flasks	Weuster-Botz[5]	5.8	N.R.	100	9	*T*, pH	Manual sampling, for OD
Parallel bubble columns	Altenbach-Rehm[6]	8	0.16	100	12	*T*, pH	Manual sampling for OD
Mini machined stirred tank	Lamping[7]	1.4	0.1	6	1	*T*	Difficult to scale
Stirred cuvette	Kostov[8]	2	0.012	1	1	*T*	Optical sensors
Gas inducing impeller	Puskeiler[11]	37	0.2–0.4	8–15	7	*T*, pH	Fed batch, Manual DO control,
Robotic fluid handling	Weuster-Botz[12]	15.2	0.2–0.4	8–15	48	*T*	at-line sensing with MTP reader
Electrolytic gas generation	Maharbiz[13]	0.5	0.04	0.25	8	*T*	Printed circuit board integration
Circular micro-channel	Quake[14]	0.9	N.R.	16×10^{-6}	6	*T*	Continuous reactors, no sensors
Passive membrane aeration	Zanzotto[16]	2.7	0.02	0.005–0.050	1	*T*	Flat form factor, no mixing
Stirred membrane aeration	Szita,[19] Zhang[18]	2.9	0.04	0.150	4	*T*	Mechanically multiplexed
Integrated microfluidics	This work	13.2	0.1	0.1	8	*T*, pH, DO	Integrated sensors and control

the highest level of performance in terms of cell density and controlled parameters. However, these systems require expensive pipetting robotics and careful sterilization of the pipette tips to prevent contamination during frequent sampling.

A lab-on-a-chip approach offers the potential for circumventing the need for robotic multiplexing, however, none of the microbioreactor systems developed to date have taken advantage of microfluidic integration to achieve parallelism. In addition, no existing lab-on-a-chip approach has succeeded, even in a single reactor, in providing the oxygen transfer rate and the pH control capabilities of stirred tank bioreactors that are required for high cell density growth.

We have used a microfabrication process that allows the integration of multiple devices in a single chip to develop a microbioreactor array capable of providing a high oxygen transfer rate ($k_La \sim 0.1\ s^{-1}$) along with dissolved oxygen and pH control. This was enabled by a flat form factor bioreactor design, with 100 μL working volume, that integrated fluid injectors and a peristaltic oxygenating mixer. Our integrated approach, with convenient to use pneumatic and optical interfaces afforded by the lab-on-a-chip format allows non-invasive sensing and actuation. This preserves the sterility inside the bioreactors, a distinct advantage over robotically multiplexed systems.

Materials and methods

Device

The microbioreactor array module (Fig. 1a) comprised four 500 μm deep growth wells with a working volume of 100 μL. Each growth well had a peristaltic oxygenating mixer, a pair of integrated fluid injectors for pH control, and integrated optical sensors for the measurement of dissolved oxygen and pH.[20] Interfacing with pneumatic actuation lines was accomplished by face sealing to gaskets molded directly onto the device (Fig. 1d), eliminating the need for plugging individual pressure lines.[22]

The peristaltic oxygenating mixer comprised membrane sections that could be deflected into the growth well by pressurizing the mixing tubes (Fig. 1b,c) using air or a gas mixture at 4 psi in a propagating pattern that approximated peristalsis: 00011, 00110, 01100, 11000, 10000, 00000, 00001, 00011, where '1' indicates pressurized and '0' indicates vented. The pressurization state was updated at 25 Hz.

The fluid injectors comprised a nominally 16 μL hemispherical fluid reservoir (Fig. 1b), and three metering valves (Fig. 1d). The fluid reservoir could be pressurized through a PDMS membrane and pressure chamber in order to drive the fluid into the well against back pressure. The metering valves were membrane pinch valves that spanned a shallow rounded injector channel. A fluid plug was injected by actuating the metering valves and pressure reservoir using the sequence 100-1, 101-1, 001-0, 011-0, 111-0, where the first three digits indicate the pressurization state of the metering valves and the last digit, the pressurization state of the reservoir.

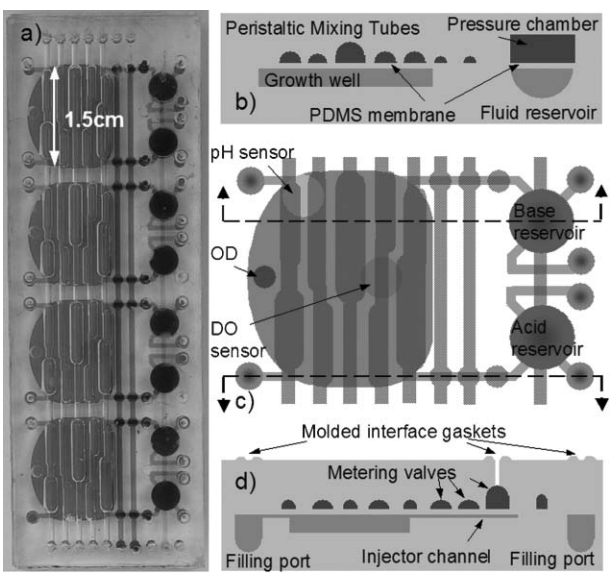

Fig. 1 Photograph and schematic of a microbioreactor array module. (a) Photograph of four reactors integrated into a single module. (b) Cross-section of a microbioreactor showing the peristaltic oxygenating mixer tubes and fluid reservoir with pressure chamber. (c) Top view of a microbioreactor showing optical sensors and layout of peristaltic oxygenating mixer and fluid injectors. Growth well is 500 μm deep, giving a 100 μL working volume. (d) Cross-section showing the fluid injector metering valves.

Actuation of the peristaltic oxygenating mixer and two of the fluid injector metering valves were shared along a module for scalability. The fluid injector valve closest to the reservoir was independently controlled, allowing independent row-column addressing of each fluid injector, which resulted in favorable scaling of the necessary pneumatic control valves.

Device fabrication

The microbioreactor array modules were fabricated from polydimethylsiloxane (PDMS, Dow Corning, Sylgard 184) using a polycarbonate mold transfer process, which allowed fabrication of the microbioreactor features with multiple depths and profiles.

Master internal molds (positive) and the external molds (negative) were fabricated in polycarbonate using a tabletop CNC milling machine (Flashcut, CNC mill 2000) with various size ball and square end mills. After machining, the molds were polished to optical clarity using a vapor of methylene chloride[23] for 3–5 seconds to remove tooling marks and scratches in order to minimize mold adhesion.

Next, negative internal molds were cast from the masters using PDMS, fully cured (65 °C, 4 h), and subsequently treated with a fluorosilane compound[24] (United Chemical Technologies, T2492), at 70 °C under 25 psig vacuum for 6 or more hours to prevent PDMS adhesion to the PDMS mold.

The device was fabricated using one PDMS internal mold and one polycarbonate external mold for the top, mixer/valve layer, and another set of molds for the bottom, base layer. External molds defined external interface features, which included ports to access the internal features, gaskets for face sealing to an external manifold, and recesses to accept fiber optics to address internal sensors. No hole punching as with previously described processes[22] was required. In addition, a PDMS membrane was spun onto a silanized silicon wafer[24] where the thickness (40–170 μm) was monitored online with an optical coherence interferometer.[25]

Optical oxygen sensors[26] were embedded into the base layer during molding and pH sensors were bonded to the inside of the growth wells after de-molding. Layers were bonded together using a partial cure bond, similar to other multilayer processes,[27] except the same 10 : 1 PDMS mixture was used for all layers. The top and bottom layers were cured for one hour at 65 °C and the membrane was cured for 20–30 minutes until it had just gelled and was tacky to the touch. At this point, the top layer was bonded to the membrane and allowed to cure for an additional 30 minutes. Then, the top layer/membrane were aligned and bonded to the bottom layer and allowed to cure for another 8 hours at 50 °C.

Bioreactor array system

The supporting system (Fig. 2b), including the pneumatic actuators, optical sensor electronics, and bioreactor control software sustains two integrated microbioreactor modules for a total of eight simultaneous bioreactions.

Pneumatic actuation was accomplished through the use of miniature 3-way solenoid switches (The Lee Co., LHDA0523111H) driven by standard driver circuits (National Semiconductor, DS3658) and a digital I/O card (National

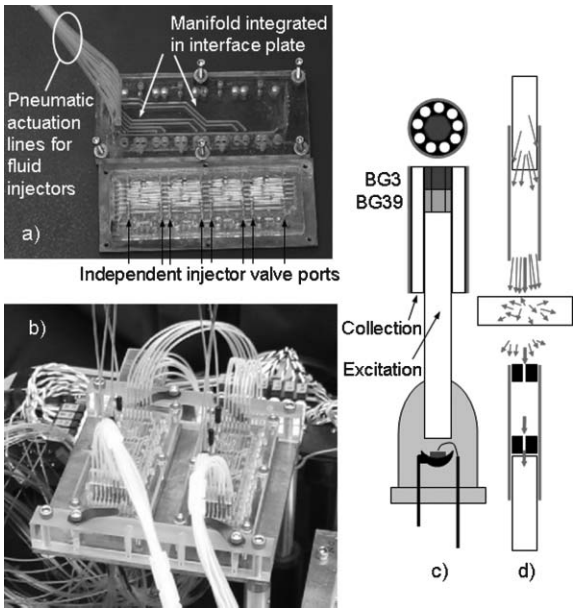

Fig. 2 Components of the system that support the microbioreactor array. (a) Photograph of interface plate with integrated manifold to route pneumatic actuation lines, face sealed to the microbioreactor module. (b) Photograph of two microbioreactor modules on a temperature controlled copper plate. Optical density excitation fibers are visible. Fiber bundles for fluorescence sensors are on the underside. (c) Schematic of a fiber bundle used to address fluorescence sensors. Excitation fibers are butt coupled to LEDs by boring a 1 mm diameter hole as close as possible to the LED die. PDMS provides index matching. (d) Schematic of the optical density measurement fibers that show the two 500 μm pinholes used to reduce the numerical aperture of the collection fiber to reject scattered light.

Instruments DAQcard-DIO-24), along with some simple digital circuitry. The interface to the microfluidic module was accomplished through a manifold integrated into a polycarbonate interface plate (Fig. 2a) that was made by CNC machining channels into a 3/16 inch thick polycarbonate sheet and thermal diffusion bonding it to a 1/16 inch thick polycarbonate sheet with drilled holes aligned to the actuation ports of the microfluidic module, allowing a simple, single step alignment and face sealing to the microbioreactor module.

Optical sensors were addressed by PMMA fiber bundles made from a central 1 mm excitation fiber (Industrial Fiber Optics, IF-C-U1000) and nine surrounding 500 μm collection fibers (IF-C-U500) (Fig. 2c). Color glass filters for the excitation (CVI Laser, BG3 and BG39) were integrated into the ends of the fiber bundles by cutting 1 mm thick color glass into hexagons inscribing a 1 mm diameter circle, using a dicing saw, and sealing them into the fiber bundles with PDMS loaded with black printer toner to absorb light that did not pass through the filters. Optical density was measured by monitoring the transmission through the flat bioreactor using low numerical aperture optics (Fig. 2d) that permitted linear correlation between optical density and cell density beyond 13 g-dcw L^{-1} (1 cm $OD_{650nm} > 40$).

The optical collection fibers terminated at red filtered photodiodes (Hammamatsu S6430-01) for the optical density and dissolved oxygen sensors and for the pH sensors at

photodiodes (Thorlabs FDS100) with a colorglass filter (CVI laser, OG530). Plastic mounts for the photodiodes allowed each photodiode to be shared by two fiber bundles. A bandpass transimpedence amplifier converted the optical signals to a voltage, which was sampled by a data acquisition card (National Instruments DAQcard-6036E). Details of the measurement techniques for pH, dissolved oxygen, optical density, and growth rate can be found in the electronic supplementary information.†

System control and signal processing for phase sensitive detection was performed using LabVIEW (National Instruments). The temperature was controlled by maintaining the copper base plate at 37 °C through a foil heater (Minco, ASI5901R10.4TFB) and an on–off temperature controller (Minco, CT325TF1A5).

Control algorithms

pH control. pH control was accomplished by intermittently injecting base or acid into the growth wells every 40–80 seconds, if necessary, to maintain the pH within a ± 0.1 deadband. The number of base injections was calculated based on the measured change in pH with time due to the metabolic processes of the growing cells, and the previous change in pH due to each injection. The injected volume varied slightly depending on how full the reservoirs were, and the back pressure due to the peristaltic mixing. The capacity of the pH control was limited by the reservoir volume (16–20 μL) and the maximum molarity of base that could be used, which was constrained by the PDMS base resistance (<2.5 M). High molarity base was found to cause bonding between the injector channel and membrane pinch valve. Increased pH control capacity was accomplished by eliminating the acid and utilizing two base reservoirs.

Dissolved oxygen control. The dissolved oxygen was controlled by varying the oxygen concentration of the peristaltic oxygenating mixer actuation gas. This was accomplished by varying the duty cycle of a solenoid valve, which alternately (0.1–3 Hz) connected the mixer pressure source with two humidification reservoirs that contained either compressed air or oxygen at 4 psi. The duty cycle of the switch was set by a proportional-integral control algorithm whose error signal was based on the minimum dissolved oxygen concentration among the four bioreactors in a module that shared a peristaltic mixer.

Escherichia coli batch culture

Escherichia coli FB21591 (*thi*C::Tn*5* -pKD46, Kan^R), obtained from the *E. coli* Genome Project at the University of Wisconsin (http://www.genome.wisc.edu), was used in all experiments. Cultures were grown in either a modified Luria-Bertani (LB) medium or defined medium at 37 °C. Inocula were prepared as described previously.[16]

The modified LB[28] consisted of (per litre): 10 g tryptone, 15 g yeast extract, 5 g NaCl, 5 g K_2HPO_4, 1.2 g $MgSO_4$, which were autoclaved, and then 1 mL trace metal solution, 100 mg Kanamycin, and 40 g glucose, were added as filter sterilized solutions. The trace metal solution contained (per litre) 4 mg $(NH_4)_6Mo_7O_{24}\cdot 4H_2O$, 71 mg H_3BO_3, 2.5 mg $CuSO_4\cdot 5H_2O$, 16 mg $MnCl_2\cdot 4H_2O$, and 3 mg $ZnSO_4\cdot 7H_2O$.

The defined medium[29] consisted of (per litre): 13.5 g KH_2PO_4, 4.0 g $(NH_4)_2HPO_4$, 1.4 g $MgSO_4\cdot H_2O$, and 1.7 g citric acid, which were autoclaved, and then 40 g glucose and 10 mL trace metal solution, were added as filter sterilized solutions. The trace metal solution was composed of (per litre 5 M HCl): 10.0 g $FeSO_4\cdot 7H_2O$, 2.0 g $CaCl_2$, 2.2 g $ZnSO_4\cdot 7H_2O$, 0.5 g $MnSO_4\cdot 4H_2O$, 1.0 g $CuSO_4\cdot 5H_2O$, 0.1 g $(NH_4)_6Mo_7O_{24}\cdot 4H_2O$, and 0.02 g $Na_2B_4O_7\cdot 10H_2O$.

Bench scale bioreactor

A fermentation with modified LB in a 4 L working volume bioreactor (Bioengineering, Type L1523) was used as a reference. During fermentation the pH was controlled at 6.9, the temperature at 37 °C, and the dissolved oxygen was maintained above 40% by adjusting the agitation speed of the impeller and also increasing the oxygen concentration in the feed gas (1 vvm) manually.

Results and discussion

Mixing

Mixing was characterized by the spread in color change of a 0.3 mM bromothymol blue solution, after an acid and base injection from the fluid injectors.[20] Mixing was complete in approximately 10–12 s with actuation conditions of 3 psi/25 Hz. The mixing time was most sensitive to actuation pressure and relatively insensitive to the actuation frequency, as indicated in Table 2. Low actuation pressures resulted in incomplete deflection of the membrane segments, which resulted in smaller fluid displacement per cycle.

Because the narrower parts of the membrane sections deflected less than the wider parts for a given actuation pressure, fluid preferentially flowed under the narrow areas, which generated fluid flow transverse to the peristalsis direction and improved lateral mixing across the growth well. A movie illustrating the mixing pattern is provided in the electronic supplementary information.†

Oxygen transfer coefficient

The definition of the oxygen transfer coefficient assumes a perfectly mixed bulk liquid and a liquid film model for air bubbles (Fig. 3a) circulating in the medium. The dissolved oxygen concentration, C, is modeled with the following equation.

$$\frac{dC}{dt} = k_L a(C^* - C) - \mathrm{OUR} \quad (1)$$

Table 2 Mixing under various actuation conditions, 70 μm thick membrane device

Actuation condition	Mixing time[a]/s
4 psi/25 Hz	6 ± 2
3 psi/25 Hz	11 ± 2
2 psi/25 Hz	30 ± 5
4 psi/40 Hz	5 ± 1
3 psi/40 Hz	9 ± 2
2 psi/40 Hz	25 ± 5

[a] Mixing times were estimated by visual inspection.

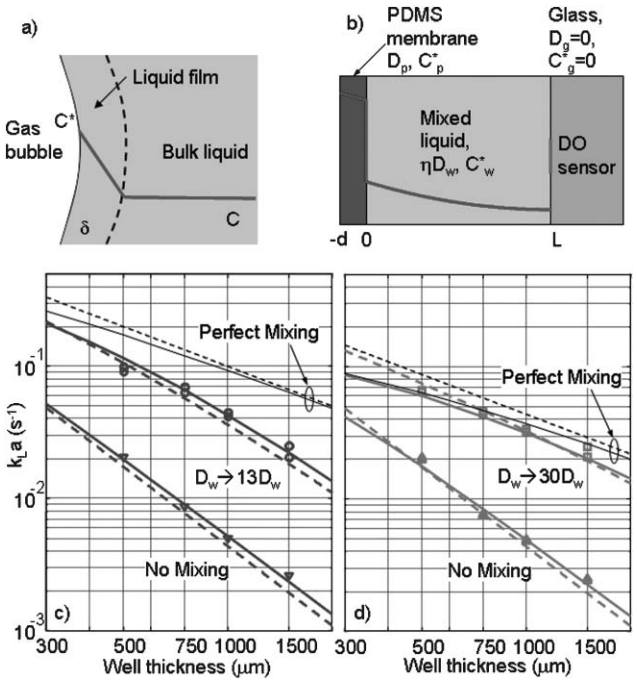

Fig. 3 Oxygen transfer coefficient models and measurements. (a) Liquid film model for stirred tank bioreactors. (b) Flat bioreactor model with PDMS membrane and growth well. (c), (d) Comparisons of k_La_{dg} measurements (markers) using dynamic gassing with theoretical values (solid lines) along with corresponding theoretical steady state k_La_{ss} (dashed lines). (c) 70 μm thick membrane, 40 Hz, 4 psi. (d) 160 μm thick membrane, 40 Hz, 8 psi.

Where the k_La captures the liquid film thickness, diffusion coefficient, and total surface area of bubbles per unit volume, C^* is the saturation concentration in the liquid for a given oxygen partial pressure, and OUR is the oxygen uptake rate. From eqn (1), we can see that measurement of the k_La using a dynamic gassing method[30] also indicates the maximum oxygen uptake rate, $OUR_{max} = k_LaC^*$, that can be supported in steady state before oxygen limitation ($C \approx 0$), which is the biologically relevant parameter.

This is not generally true for flat form factor bioreactors (Fig. 3b), where the oxygen concentration is not uniform inside the liquid. In this case, the appropriate physical model is

$$\frac{\delta C}{\delta t} = \frac{\delta}{\delta z}\left(D(z)\frac{\delta C}{\delta z}\right) - \mathrm{OUR} \tag{2}$$

where $D(z)$ is the diffusion coefficient of PDMS ($-d < z < 0$) or water ($0 < z < L$). The k_La extracted from a dynamic gassing measurement, k_La_{dg}, can be calculated by reducing eqn (2) into eqn (1) through an eigenmode expansion, keeping only the lowest order mode.[31] The k_La_{ss} corresponding to the maximum supportable OUR can be calculated by solving eqn (2) in steady state resulting in

$$k_La_{ss} = \frac{1}{\dfrac{Ld}{(D_p/K)} + \dfrac{L^2}{2D_w}} \tag{3}$$

which can be interpreted as the parallel sum of the k_La_{ss} due to the membrane and diffusion

$$k_La_{ss}\underset{mem}{} = \frac{(D_p/K)}{Ld} \tag{4}$$

$$k_La_{ss}\underset{diff}{} = 2\frac{D_w}{L^2} \tag{5}$$

where D_w (2.19×10^{-5} cm^2 s^{-1})[32] is the diffusion coefficient of oxygen in water, D_p (2.15×10^{-5} cm^2 s^{-1})[33,34] is the diffusion coefficient of oxygen in PDMS, and K (0.3) is the partition coefficient, or ratio of oxygen saturation concentrations in water, C^* (0.27 mM),[35] and PDMS, C_p^* (0.9 mM),[36] in an oxygen partial pressure of 0.21 atm.

As discussed in the electronic supplementary information,† these results are similar to those calculated dynamically through the eigenmode expansion, indicating that the k_La_{dg} derived from dynamic gassing measurements will be indicative of the maximum supported OUR.

The calculated k_La as a function of well depth for microbioreactors with 70 μm and 160 μm thick membranes are shown in Fig. 3c and d. Calculations are compared with measurements from glass bottom devices with 500 μm, 750 μm, 1000 μm, and 1500 μm depths for mixed and unmixed conditions. Imperfect mixing was modeled with an effective diffusion coefficient[37] by introducing a diffusion enhancement factor, η, such that $D_w' = \eta D_w$. A larger diffusion coefficient results in a smaller diffusion time and a more homogeneous dissolved oxygen concentration, which adequately models the effect of mixing. The best fit diffusion enhancement factors were $10 < \eta_{70\mu m} < 16$ and $20 < \eta_{160\mu m} < \infty$ for the thin and thick membranes, respectively. The results with the thick membrane were much less sensitive to mixing efficiency because the membrane contribution to the k_La was limiting. For the 70 μm thick membrane, the k_La was limited by the mixing efficiency and therefore a narrower range of $\eta_{70\mu m}$ enveloped the measured data. In this case, a higher k_La would be accessible through improvements in mixing efficiency. The difference in η between the thin and thick membranes was the result of different mixing conditions due to different membrane deflections and actuation conditions for the two devices (70 μm: 4 psi, 40 Hz, 160 μm: 8 psi, 40 Hz). Overall, the improvement in k_La due to mixing is evident, with an average 8× increase in k_La for the 70 μm thick membrane and 6.25× increase in k_La for the 160 μm thick membrane.

E. coli batch culture

A series of *Escherichia coli* fermentations were conducted with three to six replicates for each of four different growth conditions. Measurements of the cell density, pH, and dissolved oxygen, taken every 40–80 seconds, are shown in Fig. 4. The solid lines represent the average of all replicates for a given condition, with the exception of the controlled dissolved oxygen curve (Fig. 4d). In this case, the line represents the minimum dissolved oxygen among the replicates, which was the variable used for oxygen control along a microbioreactor module. The error bars indicate the maximum and minimum boundaries of the replicates for a given growth condition, and

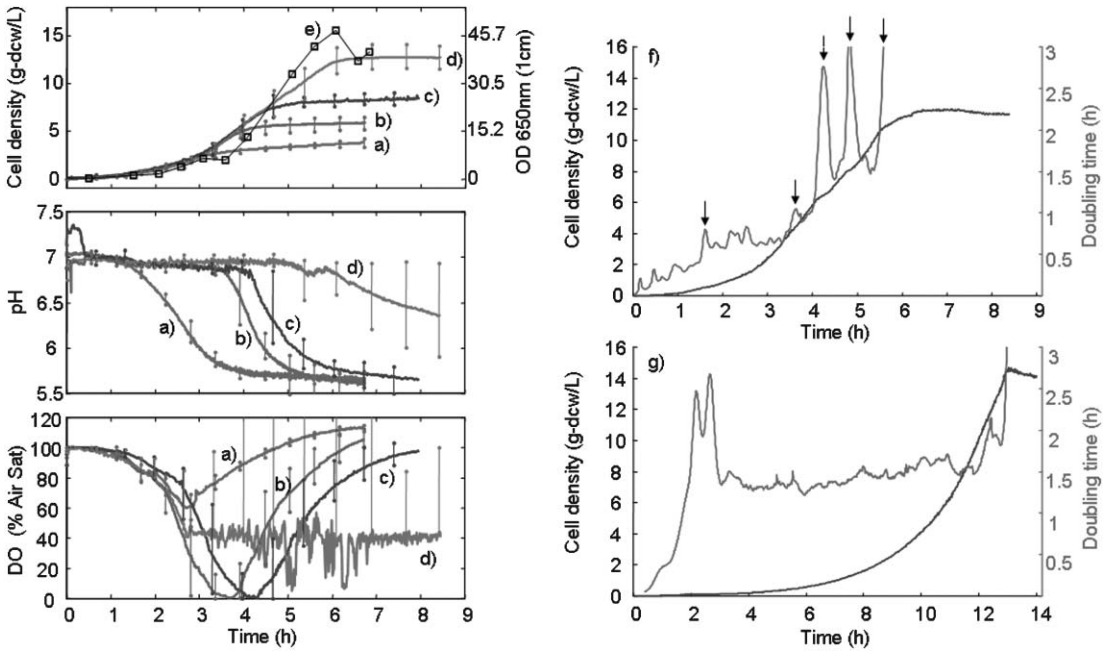

Fig. 4 Data for *E. coli* fermentations in modified Luria–Bertani medium with four different experimental conditions: (a) no pH control (red, 3 replicates); (b) pH control with 1.6 M NH_4OH (pink, 5 replicates), (c) pH control with 2.4 M NH_4OH (blue, 4 replicates), (d) pH control with two 2.4 M NH_4OH reservoirs and dissolved oxygen control set for >50% oxygen (green, 6 replicates). Solid lines indicate the mean of all replicates, with the exception of the controlled dissolved oxygen curve (green), which for clarity shows the minimum dissolved oxygen. The error bars indicate the minimum and maximum data points of all replicates. (e) Black square markers are cell density data from a 4 L bench scale fermentation. (f) Single replicate from a pH controlled fermentation on modified LB medium. Kinks in the growth curve are clearly visible at times 1.5, 3.5, 4, 5, and 6 hours which are highlighted by the change in growth rate, or as shown, the instantaneous doubling time. Such changes would not be resolvable in growth curves sampled every hour and indicate potential nutrient limitations. (g) Single replicate from a pH controlled fermentation in defined medium. Aside from the early portion of the fermentation, corresponding to the lag phase, exponential growth occurs with an approximately constant doubling time.

indicate the precision between replicates. The overlap of the growth curves for culture times less than 3 hours, where growth conditions were essentially equivalent, demonstrate reproducibility across cell cultures conducted on different days with independent inocula.

The series of experiments indicate the importance of pH control in achieving high cell densities. The longer the pH was maintained at 7, the higher the final cell density. Best results were for pH control with two 2.4 M NH_4OH reservoirs (Fig. 4d) where a maximum cell density of 13.8 g-dcw L^{-1} was achieved. The high frequency of pH control actions (>30 h^{-1}), which was enabled by the integrated microfluidic injectors, was important considering the large amount of acetate produced by this strain under excess glucose conditions. Without control, acetate secretion resulted in a sharp decrease in pH of 0.1 units every 4–5 minutes.

The steady state k_La_{ss}, could be determined from the dissolved oxygen and cell density measurements through $k_La_{ss} = OUR_{max}/C^*$ where OUR_{max} was calculated from product of the specific oxygen uptake rate (20 mmol g^{-1}-dcw h^{-1})[38] and the cell density taken when the dissolved oxygen reached zero. The oxygen saturation concentration, C^*, was assumed to be 0.21 mmol L^{-1}, the value for water at 37 °C, which is likely an overestimate due to the dissolved salts in the medium.

The average k_La_{ss} for the 9 replicates where the dissolved oxygen was not controlled was 0.1 s^{-1} with a standard deviation of 0.02 s^{-1}, which was comparable to the expected k_La_{ss} of 0.13 s^{-1}. The maximum and minimum k_La_{ss} were 0.14 s^{-1} and 0.06 s^{-1}, respectively. We hypothesize that the variation in k_La_{ss} was due to a variation in the volume of innoculum, which had an impact on the membrane deflection, and therefore the mixing efficiency of the mixer.

The high frequency, online optical density measurements allowed accurate calculation of the instantaneous growth rate or doubling time. For growth on modified LB (Fig. 4f), five distinct kinks in the growth curve, highlighted by the changes in doubling time, were resolvable. Such changes are likely due to nutrient limitations such as the consumption of amino acids in the LB medium.[3] Upon their depletion, amino acids require synthesis by the *E. coli*, resulting in a slower growth rate. In contrast, for growth on defined medium (Fig. 4g), after a three hour lag phase, exponential growth with nearly constant growth rate throughout the fermentation was observed.

Also shown in Fig. 4e is a growth curve from a 4 L fermentation, using the same modified LB medium and strain, performed in a 5.5 L stirred tank bioreactor (Bioengineering, Type L1523). The growth curve was obtained by manually taking samples every 30–60 minutes, performing dilutions, and measuring the optical density. The data points were time shifted to account for the 1.5 hour longer lag phase in the stirred tank bioreactor and correspond well to the growth curves from the integrated microbioreactor arrays grown under the same conditions, with comparable final cell densities.

Conclusions

Microfluidic integration offers a number of advantages over miniaturization of stirred tanks and robotic multiplexing for the development of parallel bioreactor systems. Simple, batch fabrication of complex mechanical functionality such as mixing and metered fluid injection enable disposable bioreactor arrays and scalability through integration. In addition, microfluidic integration opens new possibilities for device design and system functionality.

Our flat form factor bioreactor with integrated fluid injectors and peristaltic oxygenating mixer delivered a new level of performance for microfabricated bioreactor arrays. Integrated fluid injectors enabled pH control and the peristaltic oxygenating mixer provided a high oxygen transfer rate without bubbles. Bubble free oxygenation allowed near real-time online optical density measurements that permitted detailed analysis of the cell culture growth curves to resolve changes in growth rate online. This provided a valuable phenotype for study that was previously inaccessible in parallel bioreactor systems.

Our ability to conduct fermentations under controlled conditions and provide a high oxygen transfer rate resulted in the achievement of final cell densities up to 13.8 g L^{-1} in batch culture. This was comparable to cell densities achieved in a bench scale stirred tank bioreactor and more than four times higher than previously reported cell densities in microfabricated bioreactors. Such performance indicates that our array of microbioreactors has the potential to eliminate the compromise between throughput and capability in microbiology experimental design and impact both basic research and industrial bioprocess development.

Acknowledgements

We gratefully acknowledge the DuPont-MIT Alliance (DMA) for funding and Prof. Klavs Jensen for discussing the manuscript.

References

1 D. Weuster-Botz, *Adv. Biochem. Eng. Biotechnol.*, 2005, **92**, 125–143.
2 J. C. March and W. E. Bentley, *Curr. Opin. Biotechnol.*, 2004, **15**, 495–502.
3 J. Ihssen and T. Egli, *Microbiology*, 2004, **150**, 1637–1648.
4 W. A. Duetz, L. Ruedi, R. Hermann, K. O'Connor, J. Buchs and B. Witholt, *Appl. Environ. Microbiol.*, 2000, **66**, 2641–2646.
5 D. Weuster-Botz, J. Altenbach-Rehm and M. Arnold, *Biochem. Eng. J.*, 2001, **7**, 163–170.
6 J. Altenbach-Rehm, C. Nell, M. Arnold and D. Weuster-Botz, *Chem. Eng. Technol.*, 1999, **22**, 1051–1058.
7 S. R. Lamping, H. Zhang, B. Allen and P. Ayazi Shamlou, *Chem. Eng. Sci.*, 2003, **58**, 747–758.
8 Y. Kostov, P. Harms, L. Randers-Eichhorn and G. P. Rao, *Biotechnol. Bioeng.*, 2001, **72**, 346–352.
9 P. Harms, Y. Kostov, J. A. French, M. Soliman, M. Anjanappa, A. Ram and G. Rao, *Biotechnol. Bioeng.*, 2006, **93**, 6–13.
10 R. Puskeiler, A. Kusterer, G. T. John and D. Weuster-Botz, *Biotechnol. Appl. Biochem.*, 2005, **42**, 227–235.
11 R. Puskeiler, K. Kaufmann and D. Weuster-Botz, *Biotechnol. Bioeng.*, 2005, **89**, 512–523.
12 D. Weuster-Botz, R. Puskeiler, A. Kusterer, K. Kaufmann, G. T. John and M. Arnold, *Bioprocess Biosyst. Eng.*, 2005, **28**, 109–119.
13 M. M. Maharbiz, W. J. Holtz, R. T. Howe and J. D. Keasling, *Biotechnol. Bioeng.*, 2004, **85**, 376–381.
14 F. K. Balagadde, L. You, C. L. Hansen, F. H. Arnold and S. R. Quake, *Science.*, 2005, **309**, 137–40.
15 When calibrations between optical density and dry cell weight were not given, a conversion factor of 0.33 g-dcw/*A* was used to allow comparisons between systems. This assumes that optical densities were measured without the collection of scattered light, which would cause deviations from the Lambert–Beer law (ref. 21).
16 A. Zanzotto, N. Szita, P. Boccazzi, P. Lessard, A. J. Sinskey and K. F. Jensen, *Biotechnol. Bioeng.*, 2004, **87**, 243–254.
17 P. Boccazzi, A. Zanzotto, N. Szita, S. Bhattacharya, K. F. Jensen and A. J. Sinskey, *Appl. Microbiol. Biotechnol.*, 2005, **68**, 518–532.
18 Z. Zhang, N. Szita, P. Boccazzi, A. J. Sinskey and K. F. Jensen, *Proceedings of Micro Total Analysis Systems, Seventh International Conference on Miniaturized Chemical and Biochemical Analysis Systems, Squaw Valley, California, USA, 2003*, The Transducer Research Foundation, San Diego, California, October 2003, pp. 765–768.
19 N. Szita, P. Boccazzi, Z. Zhang, P. Boyle, A. J. Sinskey and K. F. Jensen, *Lab Chip*, 2005, **5**, 819–826.
20 H. L. T. Lee and R. J. Ram, *Proceedings of Micro Total Analysis Systems, Ninth International Conference on Miniaturized Systems for Chemistry and Life Sciences, Boston, Massachusetts, USA, 2005*, The Transducer Research Foundation, San Diego, California, October 2005, pp. 34–36.
21 N. L. Swanson, B. D. Billard and T. L. Gennaro, *Appl. Opt.*, 1999, **38**, 5887–5893.
22 J. W. Hong, V. Studer, G. Hang, W. F. Anderson and S. R. Quake, *Nat. Biotechnol.*, 2004, **22**, 435–439.
23 *US Pat.*, 3 684 553, 1972; *US Pat.*, 4 529 563, 1985.
24 J. R. Anderson, D. T. Chiu, R. J. Jackman, O. Cherniavskaya, J. C. McDonald, H. Wu, S. H. Whitesides and G. M. Whitesides, *Anal. Chem*, 2000, **72**, 3158–3164.
25 W. V. Sorin and D. F. Gray, *IEEE Photonics Technol. Lett.*, 1992, **4**, 105–107.
26 D. B. Papkovsky, *Sens. Actuators, B*, 1995, **29**, 213–218.
27 M. A. Unger, H. Chou, T. Thorsen, A. Scherer and S. R. Quake, *Science*, 2000, **288**, 113–116.
28 J. Shiloach, J. Kaufman, A. S. Guillard and R. Fass, *Biotechnol. Bioeng.*, 1996, **49**, 421–428.
29 F. Wang and S. Y. Lee, *Biotechnol. Bioeng.*, 1998, **58**, 325–328.
30 V. Linek, P. Benes and V. Vacek, *Chem. Eng. Technol.*, 1989, **12**, 213–217.
31 Successive eigenvalues were larger by a factor of $(2n + 1)$.
32 C. E. St. Denis and C. J. D. Fell, *Can. J. Chem. Eng.*, 1971, **49**, 885.
33 X. Lu, I. Manners and M. A. Winnik, *Macromolecules*, 2001, **34**, 1917–1927.
34 D_p was measured independently for Sylgard 184 by fitting the time response of the oxygen concentration at the bottom of 660 μm and 1525 μm thick slabs of Sylgard 184 to finite difference calculated responses. $D_p = 2.1 \times 10^{-5}$ cm^2 s^{-1} was the best fit.
35 E. Douglas, *J. Phys. Chem.*, 1964, **68**, 169–174.
36 No measurements of C_p* for Sylgard 184, a vinyl terminated, silica filled PDMS, were available. The best fit to the data C_p* = 9×10^{-4} M at 0.21 atm O_2, was consistent with reduced O_2 saturation in silica filled PDMS[33] and measured values for pure PDMS (ref. 39).
37 F. Sauges and W. Horsthemke, *Phys. Rev. A*, 1986, **34**, 4136–4143; M. N. Rosenbluth, H. L. Berk, I. Doxas and W. Horton, *Phys. Fluids*, 1987, **30**, 2636–2647.
38 K. B. Andersen and K. von Meyenburg, *J. Bacteriol.*, 1980, **144**, 114–123.
39 T. C. Merkel, V. I. Bondar, K. Nagal, B. D. Freeman and I. Pinnau, *J Polym. Sci., Part B: Polym. Phys.*, 2000, **38**, 415–434.